

1995
Bridges 1995

Quantification of Individual VOC Reactivity Using a Chemically Detailed, Three-Dimensional Photochemical Model

MICHELLE S. BERGIN,^{†,‡}
ARMISTEAD G. RUSSELL,^{*,†} AND
JANA B. MILFORD[§]

Department of Mechanical Engineering, Carnegie Mellon University, Pittsburgh, Pennsylvania 15213, and Department of Mechanical Engineering, University of Colorado, Boulder, Colorado 80309

Urban ozone reduction strategies targeting volatile organic compounds (VOCs) have focused primarily on controlling the total mass of VOC emitted, neglecting the variation in potential ozone formation by individual species. This variation in ozone potential, termed reactivity, is examined here using a three-dimensional Eulerian photochemical airshed model with a detailed chemical mechanism. Three metrics were examined to quantify the impact of individual VOCs on ozone levels; peak ozone, population-weighted exposure, and spatial-weighted exposure. Reactivities were dependent on the metric used, although the overall trends were very similar. Reactivities differed by over an order of magnitude between species. The Eulerian modeling results are compared with those of a similar study performed using a zero-dimensional model, which is the basis for reactivity quantification for alternative fuel regulations by the California Air Resources Board. The results were well correlated between models for metrics calculated at similar precursor ratios; however, notable differences in reactivity were predicted for some important species, probably due to the multi-day simulation periods and the inclusion of cloud cover by the airshed model.

Introduction

Tropospheric ozone control efforts rely on reducing emissions of nitrogen oxides (NO_x) and volatile organic compounds (VOCs), the two primary classes of ozone precursors. Most current VOC-based ozone control strategies focus on reducing total mass of VOC emissions, regardless of chemical composition except for the most unreactive species. Based on past research showing that individual

VOC species have substantially different effects on ozone formation (1, 2), a recent regulation in California incorporates reactivity values to try to focus control efforts and technology development on those species with the highest predicted ozone impacts. An additional incentive for reactivity-based regulations is the potential economic benefits (3).

Controversy has arisen over the applicability of reactivity quantification for regulatory use, especially on a national level, in part because ozone formation is dependent on local meteorology, precursor ratios, and other dynamic variables, and also because of uncertainties in the methods used to predict ozone behavior. In particular, the reactivity scale adopted for use in the California regulations was developed by applying a zero-dimensional model to a wide variety of urban conditions. While capturing a wide range of atmospheric conditions and chemical detail, there is some concern over the level of physical detail accounted for by this model and the suitability of this scale to specific airsheds.

The study presented here addresses some of these issues through the application of a three-dimensional, chemically detailed airshed model to the Los Angeles air basin. Reactivities were estimated for selected VOCs using several different measures of their impacts on basin-wide air quality. The results are compared to the previous zero-dimensional air quality model study (4) used to develop the regulatory reactivity scale.

Application of Reactivity-Based Information

A recent regulation, which is part of the Low Emission Vehicle and Clean Fuels program developed by the California Air Resources Board (5, 6), arose from interest in the use of reformulated gasoline and alternative fuels as a measure to reduce ozone in urban areas and has focused attention on attempts to quantify the reactivity of various organic compounds. This regulatory application is presented here as a specific motivation for the development of a reactivity scale for mobile source VOC emissions and also as a general example of the utilization of reactivity values. The quantification of reactivity adjustment factors (RAFTs) for alternative fuels is mandated by this regulation, where an RAF is defined as

$$RAF = \frac{\sum_{i=1}^N F_{A_i} R_i}{\sum_{i=1}^N F_{B_i} R_i} \quad (1)$$

where F_{A_i} is the mass fraction of compound i in the test fuel exhaust (alternative fuel); F_{B_i} is the mass fraction of compound i in the base fuel exhaust (conventional gasoline); and R_i is the reactivity of species i (g of ozone formed/g of compound i emitted). An RAF is the amount of ozone formed from a unit mass emission from an alternatively fueled vehicle compared to the amount of ozone formed from an equal mass of VOC emitted by a conventionally-fueled vehicle. RAFTs are designed to provide an accurate comparison of the potential ozone formation of the combustion exhaust of alternative fuels and reformulated

* Author to whom correspondence should be addressed.

[†] Carnegie Mellon University.

[‡] Present address: National Renewable Energy Laboratory, Golden, CO 80401.

[§] University of Colorado.

gasoline with respect to conventional gasoline. Without this type of adjustment, a low mass emission rate of highly reactive exhaust would appear preferable to a higher mass emission of a much less reactive set of species. As is seen below, species reactivities can vary by over an order of magnitude, so the potential to misjudge the atmospheric impact is significant if these differences are not considered.

To calculate a fuel RAF, a reliable reactivity value, R_i , must be determined for the important reactive organic species present in fuel combustion exhaust. The reactivity scale presently selected for the regulation is the maximum incremental reactivity (MIR) scale, developed by Carter (4). This scale was selected because it incorporates a wide variety of environmental conditions and tends to represent VOC behavior in highly polluted, urban areas represented by low VOC to NO_x ratios where VOC control and reactivity weighting are most effective. The MIR scale was developed using a zero-dimensional, photochemical model with a detailed chemical mechanism, Statewide Air Pollution Research Center 1990 (SAPRC90) (7). Ten-hour episodes were simulated for 39 meteorological environments representing cities or "trajectories". Each trajectory specifies the pollutant emissions and time-varying inversion heights, photolytic parameters, temperature, and humidity representative of a high ozone episode for a city. A species MIR value is the average for the 39 trajectories of the maximum increase in ozone formation over a large NO_x range, due to an increase in that species. The MIR value was obtained by adjusting NO_x inputs to where the base VOC mixture had the highest incremental reactivity.

A similar scale, developed using the same air quality model as the MIR scale, is the maximum ozone incremental reactivity (MOIR) scale (4). MOIR values are defined as the difference in peak ozone obtained throughout the simulations with base and increased VOC emissions at the NO_x conditions leading to the highest peak ozone.

The MIR and MOIR scales are of interest for comparison to the airshed model results because of the range of VOC/ NO_x ratios and meteorological trajectories incorporated by these metrics as well as the regulatory application of the MIR scale. One of the meteorological trajectories incorporated by these scales represents Los Angeles, which is the modeling domain for this study. For this reason, the MIR results for the Los Angeles trajectory, referred to as the LA MIR scale, are also included for comparison.

Issues in Reactivity Quantification

Atmospheric models of varying complexity are used to predict the nonlinear interactions of ozone precursors, which are dependent on meteorology, ambient precursor ratios, and other dynamic variables. Model complexity is weighed against computational and input requirements. Zero-dimensional models, or box models, have a low level of physical detail and so are useful in studies that require large numbers of simulations, such as that used to quantify the MIR scale and for statistical studies. Studies requiring high levels of physical detail are performed with three-dimensional air quality models, which can more fully capture complex behaviors such as ozone formation.

The effects of uncertainty, while not addressed in this paper, are important to consider when evaluating model predictions. A number of studies have been performed on the most likely sources of uncertainty, such as the emissions inventories and the chemical mechanism, for both box models (8, 9) and three-dimensional models (9-12) and

found the levels of uncertainty to be acceptable. However, even when a high correlation is shown to exist between predictions and measurements, there is a potential for compensating errors to be affecting the predictions. Other major issues of concern in the quantification of reactivity involve the reliability of the prediction of ozone formation sensitivity to local meteorology, precursor concentration ratios, and atmospheric variability. Some of these issues have also been addressed in a variety of studies using box models (2, 4, 8, 9) and a three-dimensional model (9-14).

An important issue addressed by this study is the effects of the level of physical and chemical detail accounted for by the air quality model and incorporated into the reactivity quantification metric. Box models, such as the one used to calculate the MIR scale, though valuable in examining a wide range of precursor ratios and number of chemical species, do not account for carryover effects during multi-day episodes or variations affecting population and spatial exposures. This study also addresses how reactivity metrics are affected by the geographic distribution of precursor ratios and how these differences affect the prediction agreement between various reactivity scales.

To address these issues, the SAPRC90 chemical mechanism was integrated into the Carnegie/California Institute of Technology (CIT) airshed model, a physically detailed, three-dimensional, Eulerian, photochemical air quality model. This model was then used to calculate a variety of measures of the reactivity of individual VOCs in the Los Angeles air basin. A similar study using the CIT air quality model was previously performed for 11 lumped species (13) using the LCC mechanism (15), a less detailed, older chemical mechanism. One limitation of that study is that lumped VOC species were primarily considered. Also, the results of that study were not directly comparable to the regulatory MIR scale because of the use of a different chemical mechanism. The reactivity scales chosen for presentation here, from simulation with the CIT model and the SAPRC90 mechanism, are comprised of three ozone impact measures. These measures, or metrics, are defined below. The three box model measures described previously (MIR, MOIR, and LA MIR) are also presented for comparison.

Application of the CIT Airshed Model

The CIT airshed model solves the atmospheric advection, dispersion, and reaction equation throughout a three-dimensional grid to predict the resulting pollutant concentrations both spatially and temporally and also how those concentrations respond to emissions changes (9). A chemical reaction mechanism provides the information needed to calculate the production and destruction of species. An extended chemical mechanism, SAPRC90, was integrated into the CIT model to obtain the chemical detail necessary for specific reactivity calculations. This version of the CIT model is identical to that discussed by Harley et al. (12), with the exception of the chemistry-related parameters and model inputs. SAPRC90 was chosen because it can be made chemically explicit for the initial oxidation reactions of a large number of organics and allows direct comparison with previous zero-dimensional box model studies, particularly the MIR scale specified by the RAF regulations. Table 1 shows characteristics of this mechanism as implemented.

TABLE 1
SAPRC90
Implemen

The ch
simultane
perature,
species co
accounts
required b
assumptio
to increa
SAPRC90
differenti
The Hyb
accurate,
solver of

After t
CIT pred
LCC mec
11). In t
predictio
observed
SAPRC90
the LCC-
CPU req
anism. T
mechanis

After
chosen f
or abun
tion exh
of Table
was cho
it is a se
availabl
being ir
the app
has bee
species
initial a
source
fied by
into th
well as
data co
during
which

Two
First, it
were 1
for thi
under
studie
with v
result

TABLE 1
SAPRC90 Mechanism Characteristics, As Implemented with CIT Model for Reactivity Studies

chemical species	
transported	71
steady-state	15
constant	5
explicit VOCs	33
total	91
reactions	
photolytic	20
total	203

The chemical mechanism describes a set of stiff, simultaneous differential equations dependent on temperature, pressure, photolytic conditions, and ambient species concentrations. The solution of these equations accounts for approximately 80% of the total CPU time required by the model, even though the solver used makes assumptions based on the destruction rate of each species to increase the speed of the solution. Integration of SAPRC90 into the CIT model required a verification of the differential equation solver used in the model, Hybrid (16). The Hybrid solution compared very well (9) to a highly accurate, but slower, Gear method solver, the Livermore solver of ordinary differential equations (LSODE) (17).

After testing the solver, a comparison was made of the CIT predictions with SAPRC90 to CIT predictions with the LCC mechanism, which had previously been evaluated (10, 11). In these studies with the LCC mechanism, model predictions were found to be acceptably correlated with observed concentrations. The predictions of CIT using the SAPRC90 mechanism compared very favorably to those of the LCC-based version of the model (9), although model CPU requirements almost doubled with the larger mechanism. These results support the use of a more lumped mechanism with the model when possible.

After integrating the mechanism, 27 VOC species were chosen for examination based on an expected high reactivity or abundance in alternative or conventional fuel combustion exhaust. These species are listed in the first column of Table 2. Ozone formation in the Los Angeles air basin was chosen as the initial application for this study because it is a serious air quality problem, reliable input data are available for the area, and reactivity-based regulations are being initiated in California. Also, as mentioned before, the application of the CIT model to the Los Angeles air basin has been evaluated in previous studies (10, 11). Chemical species concentrations are input to the model through both initial and boundary conditions and ground level and point source emissions inventories. Source emissions are specified by the temporal and spatial release of chemical species into the modeling domain. The emission inventories as well as other data inputs were derived from an intensive data collection period in California, August 27–29, 1987, during the South Coast Air Quality Study (SCAQS) (10), which is the simulation period for this study.

Two issues in the SCAQS inventories effect this study. First, it is generally acknowledged that the VOC inventories were underpredicted. The inventory was not enhanced for this study; however, the effect of the VOC inventory underestimation on reactivity quantification has been studied (14), and it was found that the use of two inventories with very different levels of VOC and NO_x led to very similar results. Second, many species in the emissions inventories

are lumped according to similar molecular structure or chemical behavior. For example, in the CIT version of SAPRC90, the label RCHO represents a lumped higher aldehyde class including propionaldehyde and higher aldehydes. To allow the use of the SAPRC90 mechanism with the SCAQS inventories, emission fluxes were calculated to represent SAPRC90 species classifications.

The CIT model was then applied to southern California conditions using the SCAQS base emissions inventory to obtain basecase ozone predictions. Species reactivities were developed by finding the response in ozone formation generated by using the same model with an alternative emissions inventory, which was created for each individual organic species tested. Alternative emissions inventories were created by first separating the test species from its lumped classification (if not already explicit) and then increasing the emissions of the test species proportionally to the spatial and temporal distribution of the base organic species emissions. In other words, the rates of all organic species emissions in each modeling cell are used to determine the rate of the test species emissions in that cell. A similar perturbation method was used by McNair et al. (13). The mathematical definition is shown by eq 2, where, at time *t* in model cell *x*, *y*, and *z*, the perturbed emission (*E^p*) of test species *i* is calculated as the base emission of that species (*E_i^b*) plus a fraction, *α*, of the sum of the total reactive organic gases base level emission:

$$E_i^p(x,y,z,t) = E_i^b(x,y,z,t) + \alpha \sum_j E_j^b(x,y,z,t) \quad (2)$$

Index *j* refers to each emitted VOC species. The constant fraction, *α*, was set at 20% of total emitted VOC, on a molar basis, for all organic species except carbon monoxide. Carbon monoxide emissions were increased by 100% of the total moles of VOC to account for its low reactivity. These fractions were selected because they cause a quantifiable, approximately linear effect on the ozone formation due to each species, without overwhelming the results. All other modeling factors were unchanged between simulations. Analysis was performed on the predictions for the third day of the simulation period, minimizing the residual effects of initial conditions and maximizing the ability to fully capture multi-day impacts of pollutant emissions.

Analysis Metric Definitions

One major advantage of the three-dimensional CIT model over zero-dimensional models is that a variety of air quality impacts can be defined to account for the temporal and spatial distribution of ozone, and these impacts can be combined with the human population distribution as a measure of exposure impact. Simulation results from the CIT model study were examined using various methods to quantify how the emission increases impacted ozone formation. The reactivity quantification measures consider the impact on peak ozone and on population-weighted and spatial exposure to ozone levels over 0.12 and 0.09 ppm. An averaged exposure metric is also introduced.

Peak ozone is defined simply as the maximum ozone concentration (ppm) predicted in the modeling domain using each emissions inventory. The predicted peak ozone forms relatively far downwind of Los Angeles in an area of a relatively high ratio of VOC to NO_x concentrations, which is therefore not as sensitive to VOC emissions as is most of the urban basin.

TABLE 2

Species List, Normalizing Composition, and Predicted Normalized Reactivities

	no. of carbon atoms	composite fraction (ppm of C/ppm of C)	composite normalized reactivity					
			CIT model results			box model results (6)		
			peak ozone	population exposure	spatial exposure	MIR	LA MIR	MOIR
carbon monoxide ^a	1	0.000	0.05	0.03	0.03	0.02	0.02	0.04
ethane	2	0.126	0.21	0.04	0.06	0.05	0.04	0.10
benzene	6	0.000	0.10	0.14	0.14	0.08	0.08	0.07
methyl <i>tert</i> -butyl ether	5	0.052	0.38	0.18	0.22	0.16	0.14	0.28
2,2,4-trimethylpentane	8	0.000	0.46	0.18	0.23	0.19	0.15	0.30
butane	4	0.003	0.60	0.21	0.28	0.22	0.17	0.37
methanol	1	0.000	0.54	0.32	0.30	0.26	0.23	0.34
methyl ethyl ketone	4	0.004	0.68	0.28	0.37	0.31	0.27	0.38
2-methylpentane	6	0.000	0.75	0.32	0.40	0.32	0.25	0.50
ethanol	2	0.056	0.98	0.39	0.51	0.45	0.36	0.65
ethyl <i>tert</i> -butyl ether	6	0.010	0.90	0.54	0.64	0.49	0.46	0.68
ethylbenzene	8	0.047	-0.15	0.28	0.23	0.52	0.51	0.32
toluene	7	0.060	-0.15	0.29	0.22	0.53	0.51	0.32
methylcyclopentane	6	0.141	1.24	0.58	0.74	0.58	0.48	0.84
2-methyl-1-butene	5	0.009	1.09	1.36	1.23	1.00	1.03	1.03
<i>o</i> -xylene	8	0.039	0.44	0.81	0.81	1.25	1.31	1.00
2-methyl-2-butene	5	0.055	1.29	1.61	1.52	1.31	1.27	1.25
3-methylcyclopentane	6	0.001	1.75	1.73	1.70	1.37	1.30	1.36
<i>m,p</i> -xylene	8	0.121	0.52	1.06	0.99	1.43	1.54	1.14
ethene	2	0.109	1.84	1.50	1.64	1.49	1.51	1.71
1,2,4-trimethylbenzene	9	0.035	0.81	1.78	1.42	1.72	1.93	1.38
acetaldehyde	2	0.012	2.46	1.54	1.98	1.77	1.75	1.85
isoprene	5	0.000	2.22	2.62	2.30	1.81	1.82	1.80
propionaldehyde + higher aldehydes	3	0.006	3.03	1.75	2.26	1.85	1.79	1.87
propene	3	0.009	2.18	2.13	2.18	1.93	1.93	2.05
1,3-butadiene	4	0.096	2.68	2.93	2.66	2.15	2.12	2.18
formaldehyde	1	0.011	1.38	2.56	2.69	3.13	3.55	2.41

^a These calculations account for the higher incremental addition of carbon monoxide.

Population-weighted exposure, PE, is calculated as

$$PE = \sum_{\text{hour } h} \sum_{\text{cell } g} (C_{g,h} P_g t) \quad (3)$$

where, summed over each hour h and grid cell g , the population P is multiplied by the ozone concentration C and time t , where

$$t = \begin{cases} 1 \text{ h} & \text{if } C_{g,h} > C_{th} \\ 0 & \text{if } C_{g,h} \leq C_{th} \end{cases}$$

and C_{th} is a threshold ozone concentration. The units of PE are ppm person-h. This is a potential exposure metric that does not account for personal activities, particularly time spent indoors. This metric may be sensitive to small concentration shifts in heavily populated grid cells.

Spatial exposure was defined in a similar manner to population exposure, only with a spatial rather than a population multiplier, leading to units of ppm grid-h, or ppm km²-h (one model grid cell represents 25 km²). Exposure metrics were calculated for two thresholds, 0.09 and 0.12 ppm O₃, representing the California state and national ozone standards, respectively.

The individual population metrics are susceptible to a threshold problem when the perturbation in emission causes the ozone concentration in a cell to go from just under to just over the threshold, and if that cell has a large population, the impact on the results will be large even though the actual change in concentration may have been small. For example, if two species have slightly different reactivities (or the spatial impacts are slightly different), and if for one species the ozone in a highly populated grid

cell just breaks the threshold, the population-weighted exposure above the threshold increases significantly. On the other hand, if the other species is just slightly less reactive, the ozone in that cell does not break the threshold. Also, ozone levels at or near one threshold value may respond differently than ozone levels at another location.

The concentration-shift effects as well as effects caused by changes in ozone behavior near the threshold concentrations are diminished by averaging the two different threshold metrics. This is shown by eq 4 using population exposure as an example (it also applies to spatial exposure), resulting in the average threshold population exposure, PE_{AT}:

$$PE_{AT} = \frac{PE_{C_{th}=0.09} + PE_{C_{th}=0.12}}{2} \quad (4)$$

Further, averaging the threshold metrics takes into account both ozone standards, emphasizes the more polluted grid cells, and is a more compact measure. For these reasons, the averaged metric is used for the populated and spatial exposure measures in this study rather than the individual threshold results, although the nonaveraged VOC threshold metrics and other more detailed results are presented elsewhere (9).

The absolute reactivities calculated with box models (g of O₃/g of VOC) are not directly comparable to the more complex metrics used here (13, 18). Therefore, the air quality metrics from both studies were normalized and expressed in comparable units. The reactivities are reported on a per carbon rather than mass basis to better represent the energy available from the molecules. Carbon monoxide

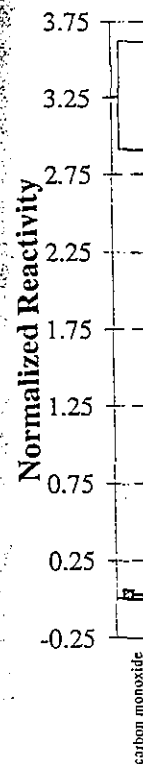


FIGURE 1. Metric

was used in the... compound, su... calculated with... species represen... was used for m... can result if t... representative... reduces uncer... reactivities (3) a... of each compo... as automobiles... Table 2, is con... present in ind... (19). Species... included in th... amounts may... Finally, the... species was ca...

$$NR_i = \frac{P_i}{P}$$

where NR_i is th... carbon based... composite, P_i is... ozone or an oz... of species i , c... is the number... or j , and f_j is... The box mo... the difference... change in oz... discussed pre...

l results (6)

MIR	MOIR
02	0.04
04	0.10
08	0.07
14	0.28
15	0.30
17	0.37
23	0.34
27	0.38
25	0.50
36	0.65
46	0.68
51	0.32
51	0.32
48	0.84
03	1.03
31	1.00
27	1.25
30	1.36
54	1.14
51	1.71
93	1.38
75	1.85
82	1.80
79	1.87
93	2.05
12	2.18
55	2.41

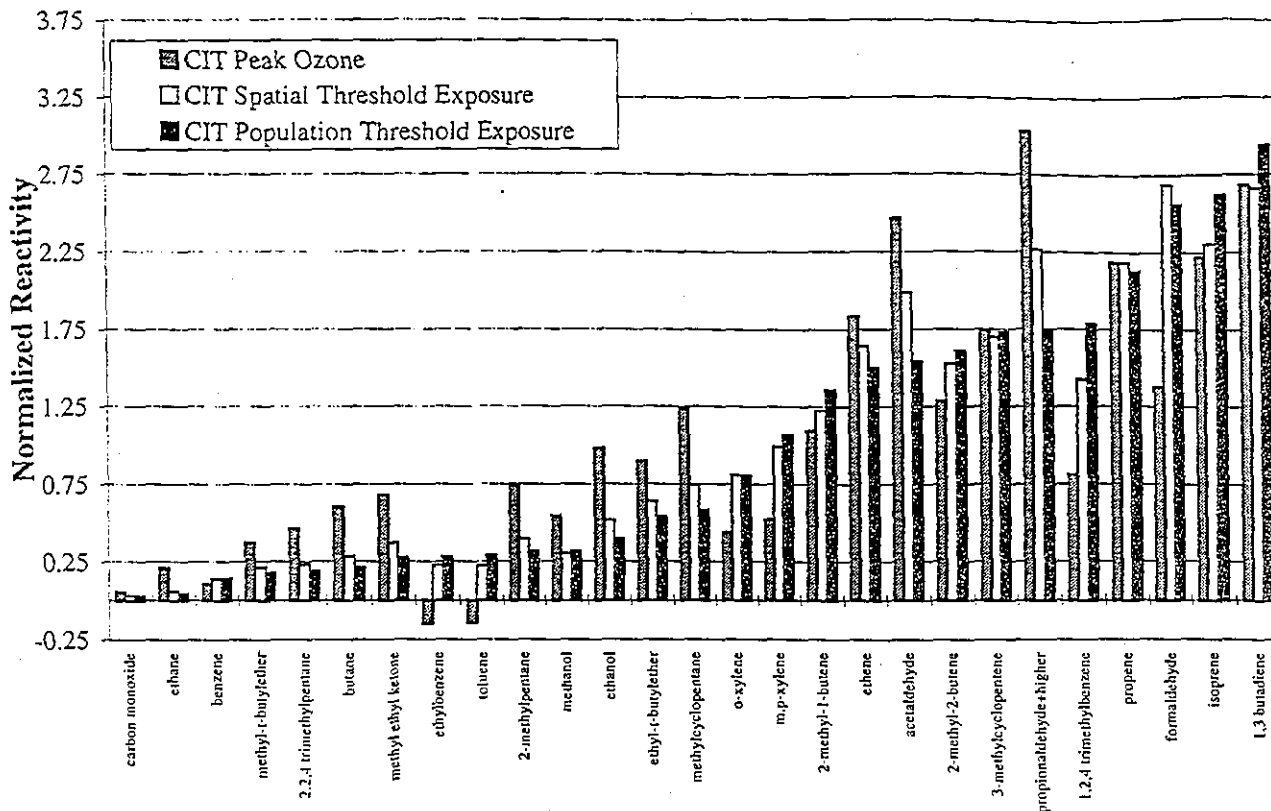


FIGURE 1. Metric comparison for CIT model results.

was used in the previous studies as the normalizing compound, such that the reactivity of each species was calculated with respect to CO. In this study, a suite of species representing the composition of automobile exhaust was used for normalizing, reducing the possible bias that can result if the normalizing species response is not representative of the majority of the compounds. It also reduces uncertainty in the calculation of the relative reactivities (3) and allows direct comparison of the reactivity of each compound to emissions from a major source, such as automobiles. The normalizing composition, shown in Table 2, is comprised of the fraction of each compound present in industry average gasoline combustion exhaust (19). Species that were not examined here were not included in the normalization composite, though small amounts may have been present in the exhaust.

Finally, the normalized reactivity of the 27 organic species was calculated for the three CIT metrics as

$$NR_i = \frac{R_i}{R_{\text{composite}}} = \frac{(P_i - P_{\text{base}}) / \text{no. of } C_i}{\sum_j \left[\frac{f_j}{\text{no. of } C_j} (P_j - P_{\text{base}}) \right]} \quad (5)$$

where NR_i is the normalized reactivity of species i , R is the carbon based reactivity of species i or the normalizing composite, P is the air quality metric of interest (e.g., peak ozone or an ozone exposure) corresponding to emissions of species i , composite species j , or the basecase, no. of C is the number of carbon atoms in a molecule of species i or j , and f_j is the carbon fraction of composite species j .

The box model reactivity measures are defined as either the difference in peak ozone (MOIR) or the maximum change in ozone concentrations (MIR and LA MIR) as discussed previously. These metrics were normalized

similarly:

$$NR_i = \frac{R_i}{\sum_j (f_j R_j)} \quad (6)$$

As shown, the normalized reactivity of species i , NR_i , is a function of the carbon-based absolute reactivity R of species i and composite species j and the carbon fraction f of the composite species j . The calculated values for all normalized reactivities are shown in Table 2.

Results and Discussion

Results for the 27 compounds for the three CIT model metrics are graphically presented in Figure 1. It is apparent that for some species the peak ozone reactivity is significantly different than the exposure-related metrics. For example, the change in peak ozone predicted for propene is higher than that for formaldehyde, while the exposure metrics both show a greater ozone impact due to formaldehyde than to propene. This holds whether considering a 0.09 or 0.12 ppm threshold and a spatial or population exposure metric.

Another interesting feature highlighted by this comparison is that the peak ozone generally predicts a higher normalized reactivity than the exposure metrics, particularly for the less reactive species, and that, in general, the spatial exposure falls between the peak ozone and the population exposure values. The photolytic and highly reactive species are the main exceptions to this ranking.

One likely major cause of these metric differences is the geographic pattern of precursor ratios in the Los Angeles basin and the sensitivity of each metric to precursor ratios. Peak ozone is a localized measure occurring in one cell,

TABLE 3

Normalized Bias and Standard Deviation between Metrics for Each Model

	norm bias	SD
CIT model		
population, spatial	-0.09	0.16
peak, spatial	0.18	0.48
peak, population	0.26	0.59
box model		
MIR, LA MIR	0.07	0.12
MIR, MOIR	-0.15	0.27
MOIR, LA MIR	0.22	0.37

whereas the exposure measures contain a larger number of cells, thereby capturing a wider range of VOC/NO_x ratios. The largest reactivity differences are found between the peak ozone and the population exposure metrics. The highly populated areas are located in the NO_x-rich regions of the South Coast air basin (12, 20), in contrast to the peak ozone concentrations which occur downwind of the core Los Angeles area and, while still VOC sensitive, is a more NO_x-lean environment than the wider Los Angeles area. The spatial exposure measure generally falls between the other metrics, accounting for ozone concentrations throughout a large portion of the domain.

A reverse in metric ranking is found for the photolytic species, likely because of the different effects of cloud cover on each metric. The peak ozone predicted reactivity is significantly lower than the exposure-related predictions, indicating a higher sensitivity to the attenuation of incident radiation. Cloud cover effects are discussed in more detail below.

Also observed in Figure 1 are the slightly negative peak ozone reactivities of ethylbenzene and toluene. These species are precursors to PAN, PPN, and other organic nitrates, which act as NO_x sinks. Since the peaks occur in a region sensitive to both VOCs and NO_x, conversion of NO_x into an organic nitrate tends to reduce peak levels of ozone in the modeling domain, in contrast with species that do not lead to the formation of such compounds. In the box model study, negative MIR or MOIR values were not observed for these species; however, the box model base peak scale (i.e., without NO_x adjustment) does show negative reactivities for toluene in some scenarios (21). Also, a negative toluene MOIR was calculated when the carbon bond 4 chemical mechanism was used with the box model (21).

To quantitatively examine the agreement between the reactivity scales, the normalized bias between metrics *x* and *y* (from either model), NB_{*x,y*}, was calculated as

$$NB_{x,y} = \frac{1}{25} \sum_{i=1}^{25} RR_{i,x,y} = \frac{1}{25} \sum_{i=1}^{25} 2 \left(\frac{R_{i,x} - R_{i,y}}{R_{i,x} + R_{i,y}} \right) \quad (7)$$

Here, RR_{*i,x,y*}, the reactivity ratio, is a function of the predicted reactivity, *R*, for species *i* from the metrics *x* and *y*. NB_{*x,y*} is the average of these reactivity ratios predicted by the metrics for 25 of the 27 species. Ethylbenzene and toluene values are omitted in this comparison because the negative results from the CIT peak ozone metric led to the denominator approaching zero. The standard deviation of the normalized bias was also calculated for the 25 species.

Table 3 shows the normalized bias and its standard deviation for comparison of metrics calculated from either

TABLE 4

Normalized Bias and Standard Deviation between Metrics and Models

box model	CIT model					
	population exposure		spatial exposure		peak ozone	
	norm bias	SD	norm bias	SD	norm bias	SD
MIR	0.04	0.22	0.13	0.25	0.30	0.60
LA MIR	0.11	0.25	0.20	0.35	0.36	0.68
MOIR	-0.11	0.35	-0.03	0.21	0.17	0.40

the CIT or box model, while Table 4 shows the same values for comparison of metrics between the models. The normalized bias and standard deviation ranges are very similar within models, with slightly higher deviations between CIT scales. The closest agreement for the CIT predictions is found between the exposure-based metrics and for the box model is found between the incremental scales.

Overall, as shown in Table 4, the normalized bias and standard deviation ranges between the box model and CIT model results were not much greater than the ranges arising from the metrics calculated within the CIT model. Across models, the population exposure results agree best with the MIR scale, while the spatial exposure results agree best with the MOIR scale, supporting the apparent sensitivity of the metrics to ozone precursor ratios. The average initial VOC/NO_x ratio was 5.8 for the box model MIR results, and the LA trajectory had a VOC/NO_x ratio of 7.6. On the other hand, the peak ozone results, which agree best with the MOIR scale, are found well downwind of Los Angeles, and while still in a VOC-sensitive location it is much less NO_x-rich, more similar to the conditions leading to the MOIR. The spatial exposure metric also includes this less NO_x-rich, high ozone region, leading to closer agreement with the MOIR scale than the MIR or LA MIR scales.

Better correlation may have been expected with the LA MIR scale than with the general MIR scale because the CIT application was also for LA conditions; however, this is not the case because the box model-calculated reactivity scales also exhibit sensitivity to precursor ratios. The CIT model metrics capture a wide variety of precursor ratios in the modeling domain, while the LA MIR has only one ratio, and the general MIR is averaged over 39 ratios. Probably for this reason, all the CIT results show better agreement with the box model MIR scale than with the LA MIR scale, although the population exposure shows better agreement with the LA MIR than the spatial exposure shows with the MIR.

In the interests of brevity, this paper focuses on the better correlated measures between the models. However, it is important to note that because of differences in behavior of various metrics, potential limitations exist in the use of any one reactivity scale. In support of a previous box model study conclusion (4), it is also noted here that a more complete understanding arises from the examination of a number of metrics.

Figures 2-4 show more detailed comparisons for the better correlated metrics across models, i.e., the MIR to exposure and MOIR to spatial exposure and peak ozone scale relations. The LA MIR scale is also included with Figure 4. Figure 2 shows the relationship between the predicted reactivities for 25 species, defined as RR_{*i,x,y*} in eq 7, for five metric pairs.

$$2((R_{x,i} - R_{y,i}) / (R_{x,i} + R_{y,i}))$$

FIGURE 2. No

The outli
ozone-based
are {CIT Pea
MOIR}. The
lower end o
MOIR} pair
of reaching
reactivity sca
little bias. TI
and {CIT Pe
m,p-xylene,
xylenes and
tolytic becau
undergo pho

The expo
grouped ne
throughout t
is usually po
reversed). T
for benzene,
the same ph
more reactiv
were not inc
previously.

The {CIT
for increme
Spatial-MOIR
metric scale
change in b
are clear fr
systematic t

To furthe
scales, regre
includes all
the previou
scales, are s

etween

peak ozone	
mean bias	SD
0.30	0.60
0.36	0.68
0.17	0.40

same values
models. The
as are very
deviations
for the CIT
ed metrics
incremental

and bias and
del and CIT
ages arising
del. Across
e best with
agree best
sensitivity
age initial
results, and
n the other
st with the
angeles, and
n less NO_x-
the MOIR.
less NO_x-
ment with
s.

with the LA
use the CIT
this is not
ivity scales
CIT model
tios in the
one ratio,
Probably
agreement
MIR scale,
agreement
vs with the

n the better
wever, it is
n behavior
the use of
box model
at a more
nation of a

ons for the
he MIR to
peak ozone
luded with
etween the
RR_{i,x,y} in eq

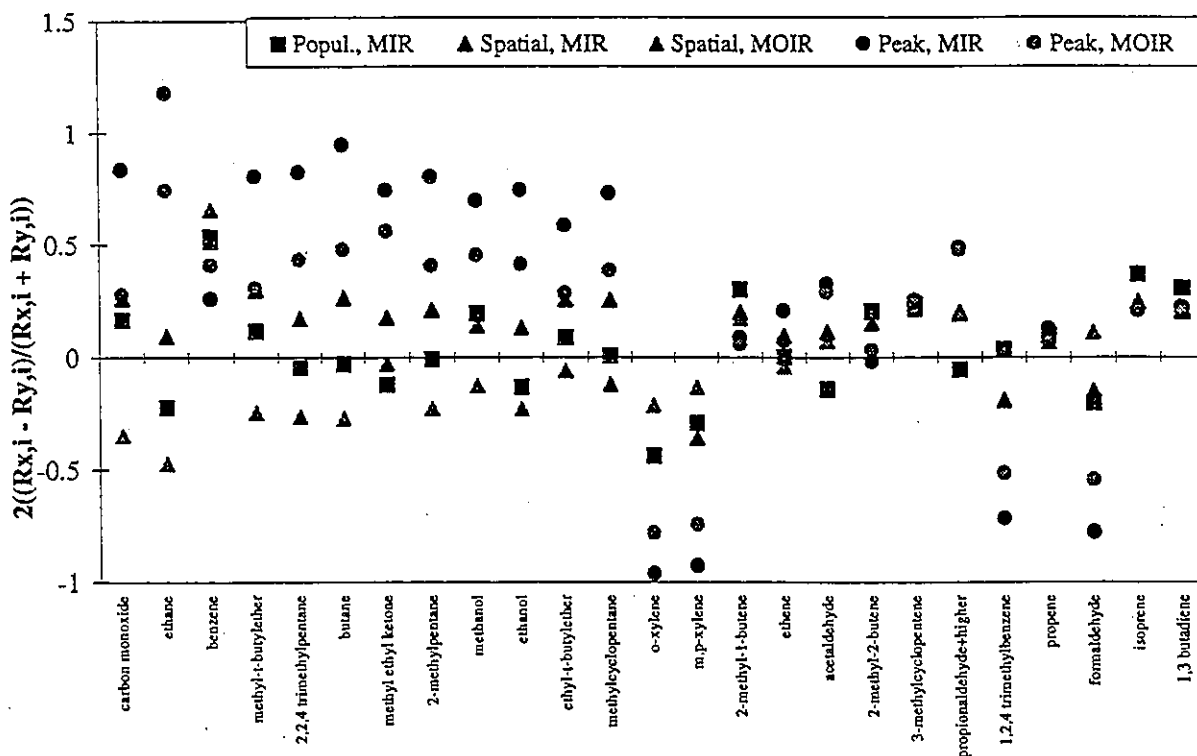


FIGURE 2. Normalized bias between reactivity metrics.

The outliers observed in Figure 2 all include a peak ozone-based metric in the calculation, i.e., the outlier pairs are {CIT Peak-MIR}, {CIT Peak-MOIR}, and {CIT Spatial-MOIR}. The three pairs all show the least agreement at the lower end of the reactivity scale, with the {CIT Spatial-MOIR} pair opposite in sign. All three show a clear trend of reaching better agreement at the higher end of the reactivity scale, where they are fairly well grouped and show little bias. The exceptions, particularly for {CIT Peak-MIR} and {CIT Peak-MOIR}, are the photolytic species, *o*- and *m,p*-xylene, 1,2,4-trimethylbenzene, and formaldehyde. The xylenes and 1,2,4-trimethylbenzene are considered photolytic because the intermediates in the oxidation pathways undergo photolysis.

The exposure to MIR comparisons are more closely grouped near zero bias and show better agreement throughout the scale, although the {CIT Spatial-MIR} bias is usually positive (negative if the order of metrics were reversed). The extremes for these two ratios are observed for benzene, which is less reactive in the box model, and the same photolytic species mentioned above, which are more reactive in the box model. Ethylbenzene and toluene were not included in this figure for the reasons discussed previously.

The {CIT Popul.-MIR} pair shows the greatest agreement for incremental metrics across models, while the {CIT Spatial-MOIR} pair shows the greatest agreement for peak metric scales. {CIT Spatial-MOIR} also shows the least change in bias for the photolytic species. These relations are clear from Table 4; however, Figure 2 exposes the systematic trend in the {CIT Spatial-MOIR} pair.

To further examine the quantitative relationship between scales, regression analysis was also conducted. This analysis includes all of the 27 species. These results, which reinforce the previous conclusions as to the agreement between scales, are shown in Table 5.

TABLE 5

Regression Results for Exposure vs MIR and Peak Ozone vs MOIR Measures

	R ²	slope	intercept
population to MIR	0.88	1.02	0.00
MIR to population		0.86	0.12
spatial to MIR	0.91	1.02	0.03
MIR to spatial		0.89	0.07
peak to MOIR	0.74	1.05	0.03
MOIR to peak		0.71	0.23
spatial to MOIR	0.97	1.19	-0.12
MOIR to spatial		0.82	0.13

A comparison of the MOIR scale with the CIT peak ozone and spatial exposure scales is shown in Figure 3, with the species arranged in order of ascending CIT peak ozone reactivity values. This comparison shows very close scaled agreement, with the exceptions of photolytic species and certain aromatics for peak ozone. The photolytic species, particularly *o*- and *m,p*-xylene, 1,2,4-trimethylbenzene, and formaldehyde, agree very well for the MOIR and spatial exposure metrics, although the predicted peak ozone reactivity is lower. Ethylbenzene and toluene have a negative peak ozone metric reactivity.

The differences in the photolytic species are likely due to the assumption of a clear-sky condition with the box model, while cloud cover measurements are used with the CIT airshed model. Within the scales predicted using the CIT model, the peak ozone reactivity metric is more attenuated for these species than the exposure metrics, as can be seen in Figure 1. This creates a larger discrepancy from the box model scales for the peak ozone predictions. With less incident sunlight, photosensitive species exhibit lower ozone impacts. The reduction in photolysis is taken directly from observations and is highly variable throughout the basin, ranging from 0 to 70%. An interesting future study would be to remove cloud cover from the model and

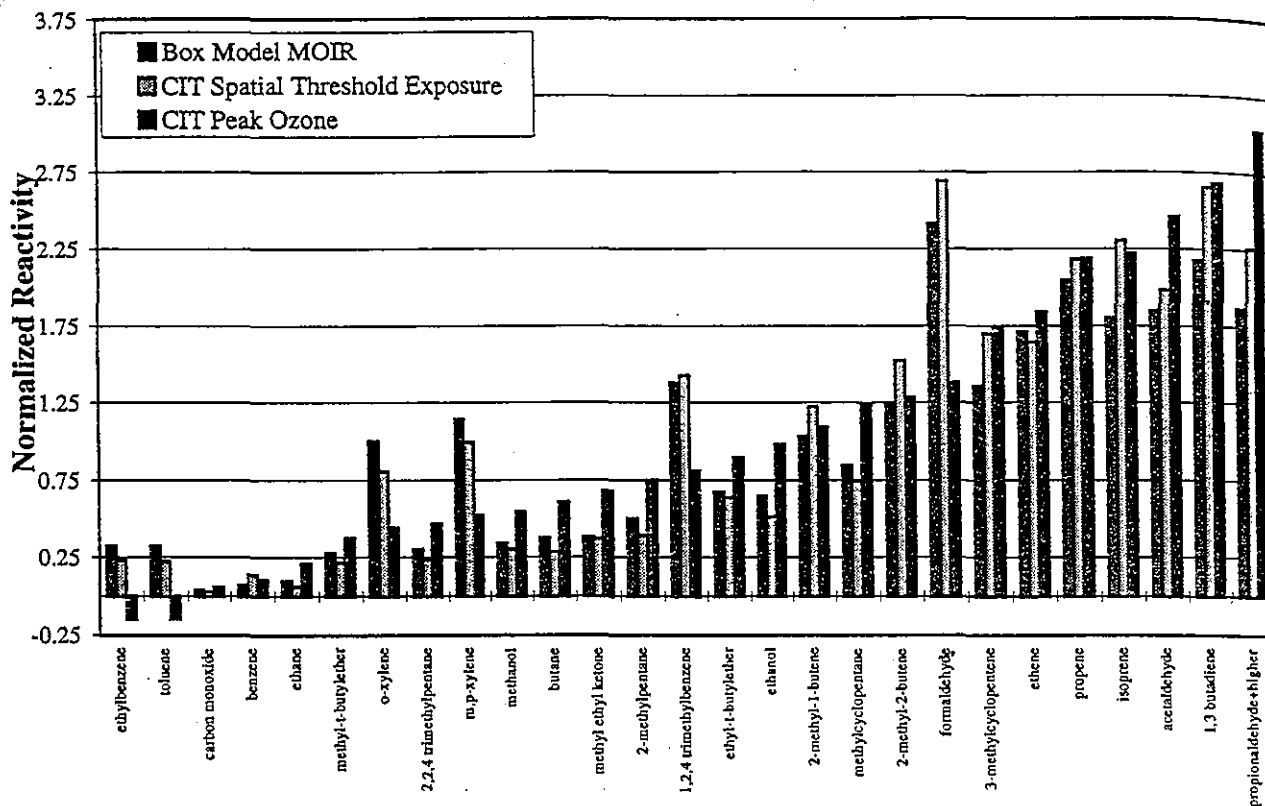


FIGURE 3. MOIR, peak ozone, and spatial exposure results.

repeat the reactivity simulations for the photolytic species. In a study of reactivity sensitivities and uncertainties, calculated reactivities were investigated by varying the photolysis rate of the aldehydes and the photolytic aromatic reaction products. The reactivities of these species were shown to be very sensitive to the photolysis parameters (9).

The two negative reactivities mentioned above, for ethylbenzene and toluene, are not predicted by the box

model, probably because the box model does not account for multi-day transport, leading to relatively lower NO_x levels. However, as mentioned previously, the box model did predict a negative MOIR when applied with a different chemical mechanism. The otherwise close agreement between the CIT peak ozone and the MOIR scales in Figure 3 may indicate a low environmental variability for peak ozone response.

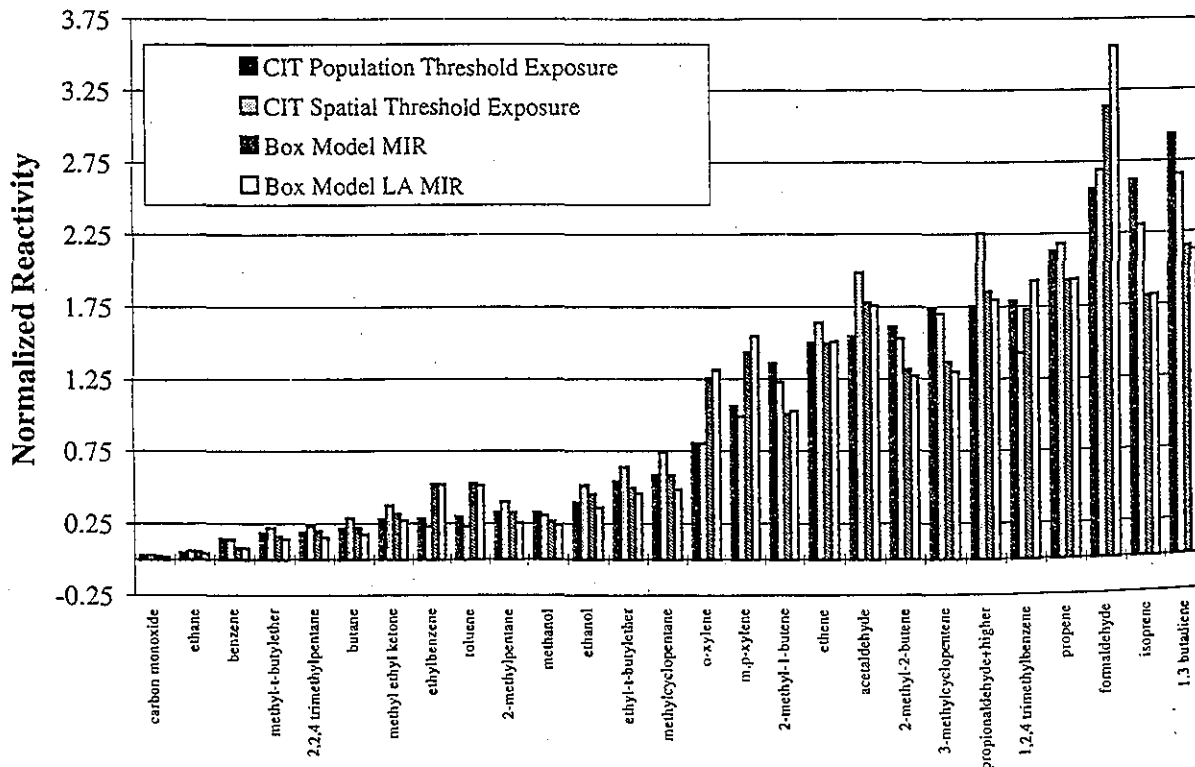


FIGURE 4. Incremental and exposure metric comparison.

Another model surface defined metrics specified three metrics. Figure 3 shows that with the MIR, the results were more or less similar to those with the MOIR. The results are again more similar to those with the MOIR in comparison. The results of the comparison of strategies for peak ozone.

While the reactivities of the species are similar, Toluene, ethylbenzene, and other aromatic aldehydes were found to have lower reactivities in the box model. In comparison to the MOIR, aromatic aldehydes were found to have lower reactivities in the box model. The peak metrics may be linked to the results of the airshed model. The results of the clear-sky model.

Summarizing the results, the comparison between the box model and the MOIR, despite the differences in the results for toluene, and ethylbenzene, according to the results of the box model, because of the higher reactivity of exhaust from the box model calculation. The results of the box model calculation are important due to the differences in the results of the conventional model. The results of the box model calculation are important due to the differences in the results of the conventional model. The results of the box model calculation are important due to the differences in the results of the conventional model.

The degree of response to the MOIR is important for the comparison of the results of the box model and the MOIR. The results of the box model calculation are important due to the differences in the results of the conventional model. The results of the box model calculation are important due to the differences in the results of the conventional model.

In summary, the results of the box model calculation are important due to the differences in the results of the conventional model. The results of the box model calculation are important due to the differences in the results of the conventional model. The results of the box model calculation are important due to the differences in the results of the conventional model.

Another measure of interest is the three-dimensional surface defined by ozone concentrations exceeding a specified threshold, represented by the CIT exposure metrics. Figure 4 is a comparison of the CIT exposure results with the MIR and LA MIR scales. The same species that were more or less reactive in the peak comparison to MOIR are again more or less reactive in the exposure to MIR comparison. This consistency is important for consideration of strategies to reduce exposure as well as for reducing peak ozone.

While the overall correlation of the MIRs and exposure reactivities is quite good, the same exceptions stand out. Toluene, ethylbenzene, and the two xylene species had lower reactivities as found by the airshed model in comparison to the box model MIRs. Likewise, some aldehydes were also less reactive. The aldehydes undergo direct photolysis, and the fragmentation products of aromatic oxidation reactions are highly photolytic. As with the peak metric scales, these discrepancies can probably be linked to the use of a reduced photolysis rate in the airshed model to account for cloud cover, as opposed to the clear-sky conditions in the box model.

Summarizing for all metrics, some apparent differences between the box model and CIT model results are notable, despite the high overall correlation. The two xylenes, toluene, and ethylbenzene have relatively high reactivities according to the box model results. These stand out because xylenes contribute substantially to the reactivity of exhaust from gasoline-fueled vehicles. Formaldehyde, which also had somewhat higher reactivities in the box model calculations than the airshed calculations, is important due to its high reactivity and presence in M85- and conventionally fueled automobile exhaust. These differences are apparently due in part to the use of different photolysis rates by the two models. The sensitivity of calculated reactivities to the chemical mechanism photolytic parameters is consequently an important interaction to be considered.

The degree of agreement between scales is generally responsive to the ozone precursor ratios. For the box model, the MOIR occurs at a higher VOC:NO_x ratio than the MIR, and for the CIT model, the peak ozone occurs downwind from the populated region, at a higher VOC:NO_x ratio. Most likely for this reason, the CIT peak ozone scale agrees best with the MOIR scale, while the CIT population exposure scale agrees best with the MIR scale. The spatial exposure metric captures the entire domain but is somewhat dominated by the higher ozone concentrations downwind of the most heavily populated region and, consequently, agrees best with the MOIR scale.

In summary, reactivities were found to differ between species by over an order of magnitude, as in previous studies conducted with airshed models as well as box models. The correlation between the box model reactivities and those calculated with the airshed model for exposure metrics was high. Airshed reactivities based on peak ozone were significantly different from those based on exposure metrics and from the box model MIRs; however, with a few exceptions, the peak ozone-based reactivities were well correlated with box model MOIRs. This is most likely because a large fraction of the population resides in the western half of the basin, where conditions are relatively NO_x-rich, while the predicted peak ozone concentrations occur further east, where conditions are richer in VOCs. The spatial exposure predictions generally fell between the two box model values. Box model-calculated MIRs correspond well to the South Coast Air Basin population exposure reactivity measures for the same reason. Overall, the results were surprisingly consistent between models

and metrics, suggesting that reactivity adjustments can be utilized in ozone control strategy decisions.

Acknowledgments

This work was performed under the sponsorship of the National Renewable Energy Laboratory (NREL) of the U.S. Department of Energy, the Auto/Oil Air Quality Improvement Research Program, and the National Aerosol Association. The views expressed in this paper are those of the authors and do not necessarily represent the views of the sponsors. Some computing resources were provided by the Pittsburgh Supercomputing Center, and we would like to thank Erik Riedel from the Computer Science Department of Carnegie Mellon University for his computer resource management.

Literature Cited

- (1) Carter, W. P. L. *Development of Ozone Reactivity Scales for Volatile Organic Compounds*; Report to the U.S. EPA, Contract CR-814396-01-0; Statewide Air Pollution Research Center, University of California: Riverside, CA, Nov 1990.
- (2) Carter, W. P. L.; Atkinson, R. *Environ. Sci. Technol.* 1989, 23, 864.
- (3) Russell, A. G.; et al. *Science* 1995, 269, 491.
- (4) Carter, W. P. L. *Air Waste* 1994, 44, 881.
- (5) California Air Resources Board. *Proposed Regulations for Low-Emission Vehicles and Clean Fuels: Staff Report and Technical Support Document*; State of California Air Resources Board: Sacramento, CA, Aug 1990.
- (6) California Air Resources Board. *Development and Evaluation of Ozone Reactivity Scale for Low-Emission Vehicles and Clean Fuel Regulations*; State of California Air Resources Board: Sacramento, CA, Apr 1992.
- (7) Carter, W. P. L. *Atmos. Environ.* 1990, 24A, 481.
- (8) Yang, Y.; et al. *Environ. Sci. Technol.* 1995, 29, 1336.
- (9) Yang, Y.; et al. *Quantification of Organic Compound Reactivities and Effects of Uncertainties in Rate Parameters*; Report to the Auto/Oil Air Quality Improvement Program under Coordinating Research Council, Inc., Contract AQIRP-19-92, Aug 1994.
- (10) Harley, R. A.; et al. *Continued Development of a Photochemical Model and Application to the Southern California Air Quality Study (SCAQ) Intensive Monitoring Periods: Phase I*; Report to the Coordinating Research Council under Project SCAQS-8; Carnegie Mellon University: Pittsburgh, PA, and California Institute of Technology: Pasadena, CA, 1992.
- (11) McNair, L. A.; et al. *Continued Development of a Photochemical Model and Application to the Southern California Air Quality Study (SCAQ) Intensive Monitoring Periods: Phase II: Model Application to the June 24-25 and December 10-11 Periods Report to the Coordinating Research Council under project SCAQS-8*; Carnegie Mellon University: Pittsburgh, PA, and California Institute of Technology: Pasadena, CA, 1992.
- (12) Harley, R. A.; et al. *Environ. Sci. Technol.* 1993, 27, 1638.
- (13) McNair, L. A.; et al. *J. Air Waste Manage. Assoc.* 1992, 42 (2), 174.
- (14) McNair, L. A.; et al. *Air Waste* 1994, 44, 900.
- (15) Lurmann, F. W.; et al. *A Surrogate Species Chemical Reaction Mechanism for Urban-Scale Air Quality Simulation Models*; 600/3-87-014; U.S. Environmental Protection Agency: Research Triangle Park, NC, Jun 1987.
- (16) Young, T. R.; Boris, J. P. *J. Phys. Chem.* 1977, 81, 2424.
- (17) Hindmarsh, A. C. *ACM-SIGNUM News.* 1980, 15 (4), 971.
- (18) Russell, A. G.; et al. *Science* 1990, 247, 201.
- (19) Croes, B. Personal communication, State of California Air Resources Board, Sacramento, CA, 1993.
- (20) Milford, J. B.; et al. *Environ. Sci. Technol.* 1989, 23, 1290.
- (21) Carter, W. P. L.; et al. *Atmospheric Process Evaluation of Mobile Source Emissions*; Final Report to the National Renewable Energy Laboratory, Subcontract XCC-4-14161-01, Dec 1994.

Received for review March 24, 1995. Revised manuscript received July 12, 1995. Accepted July 13, 1995.*

ES950204T

* Abstract published in *Advance ACS Abstracts*, September 1, 1995.